

# Relaxation behavior of polymer blends with complex morphologies: Palierne emulsion model for uncompatibilized and compatibilized PP/PA6 blends

Dean Shi <sup>a,b,\*</sup>, Guo-Hua Hu <sup>c,d,\*</sup>, Zhuo Ke <sup>e</sup>, R.K.Y. Li <sup>a</sup>, Jinghua Yin <sup>e</sup>

<sup>a</sup> Department of Physics and Materials Science, City University of Hong Kong, Tat Chee Avenue, Kowloon, Hong Kong, People's Republic of China

<sup>b</sup> Faculty of Chemistry and Material Science, Hubei University, Wuhan 430062, People's Republic of China

<sup>c</sup> Laboratory of Chemical Engineering Sciences, CNRS-ENSIC-INPL, 1 rue Grandville BP 451, 54001 Nancy, France

<sup>d</sup> Institut Universitaire de France, Maison des Universités, 103 Boulevard Saint-Michel, 75005 Paris, France

<sup>e</sup> State Key Laboratory of Polymer Physics and Chemistry, Changchun Institute of Applied Chemistry, Chinese Academy of Sciences, Changchun 130022, People's Republic of China

Received 28 December 2005; received in revised form 24 April 2006; accepted 25 April 2006

## Abstract

This paper deals with the dynamic rheological behavior of polypropylene/polyamide6 (PP/PA6) uncompatibilized blends and those compatibilized with a maleic anhydride grafted PP (PP/PP-g-MAH/PA6). The terminal relaxation times of the blends predicted by the Palierne emulsion model were compared with those obtained from experimental relaxation time spectra. The Palierne model succeeded well in describing PP/PA6 uncompatibilized blends with relatively low dispersed phase contents (10 wt%) and failed doing so for those of which the dispersed contents were high (30 wt%). It also failed for the compatibilized ones, irrespective of the dispersed phase content (10 or 30 wt%) and whether or not interface relaxation was taken into consideration. In the case of the uncompatibilized blend with high dispersed-phase content, interconnections among inclusions of the dispersed phase were responsible for the failure of the Palierne model. As for the compatibilized blends, in addition to particle interconnections, the existence of emulsion-in-emulsion (EE) structures was another factor responsible for the failure of Palierne model. A methodology was developed to use Palierne emulsion model upon taking into account the effects of the EE structure on the viscosity of the continuous phase and the effective volume fraction of the dispersed phase.

© 2006 Elsevier Ltd. All rights reserved.

**Keywords:** Polymer blends; Rheology; Relaxation time

## 1. Introduction

An immiscible polymer blend typically has a morphology in which droplets of one phase are dispersed in another one. Adhesion between the two phases is usually weak because of high interfacial tension and weak entanglements. It can be improved by the presence of a block, graft or random copolymer that tends to accumulate preferentially at the interfaces [1–3]. Rheology is one of the most frequently used methods for characterizing interfacial properties such as interfacial tension and strength [4,5] that are necessary for predicting the mechanical properties of immiscible

polymer blends. In fact, over the last decades rheological properties of immiscible polymer blends have been extensively studied from both theoretical and experimental points of view [6–35]. A rheological characteristic of such materials is an increase in elasticity at low deformation frequencies. For example, Riemann et al. [28,34] and Jacobs et al. [36] observed a slow relaxation process in small amplitude oscillatory shear experiments on a PS/PMMA blend with a compatibilizer of various molecular architectures.

Rheological studies on the interfacial properties of immiscible polymer blends rely on a key principle that such materials are emulsions in the molten state. One of the most striking properties of emulsions is that particles change shapes under a shear stress. The balance between the two types of forces exerted on the particles, viscous forces and Laplace pressure originating from the interfacial tension, dictates their equilibrium form. The process during which a deformed particle is regaining its spherical form is called the form relaxation process. This process has a characteristic relaxation

\* Corresponding authors. Address: Laboratory of Chemical Engineering Sciences, CNRS-ENSIC-INPL, 1 rue Grandville BP 451, 54001 Nancy, France. Tel.: +33 383175339; fax: +33 383322975.

E-mail addresses: [deanshi2001@yahoo.com](mailto:deanshi2001@yahoo.com) (D. Shi), [hu@ensic.inpl-nancy.fr](mailto:hu@ensic.inpl-nancy.fr) (G.-H. Hu).

time  $\tau_1$ , the form relaxation time. It is longer than the terminal relaxation time of each of the blend components.

Taylor extended Einstein's analysis to include the case of emulsions composed of spherical particles of a Newtonian liquid in another immiscible Newtonian liquid and proposed the following equation [37] that relates the viscosity of the blending system,  $\eta_b$ , to that of the medium,  $\eta_m$ :

$$\eta_b = \eta_m \left[ 1 + \left( \frac{5K + 2}{2K + 2} \right) \phi_i \right] \quad (1)$$

where  $K = \eta_d/\eta_m$ , the viscosity ratio between the dispersed phase and the medium;  $\phi_i$  is the volume fraction of the dispersed phase. Eq. (1) is reduced to Einstein's equation when  $K$  becomes infinite. Oldroyd [38] extended the above Taylor's equation to:

$$\eta_b = \eta_m \left[ 1 + \phi_i \frac{5K + 2}{2(K + 1)} + \phi_i^2 \frac{(5K + 2)^2}{10(K + 1)^2} \right] \quad (2)$$

Schowalter et al. [39] and Scholz et al. [40] extended Taylor's theory and introduced the deformability of the dispersing particles. When a dispersed system is subjected to a steady shear flow of shear rate  $\dot{\gamma}$ , the shear stress that tends to deform particles is  $\eta_m \dot{\gamma}$ . On the other hand, the interfacial stress,  $\alpha/R$  ( $\alpha$  is the interfacial tension,  $R$  is the radius of the dispersed particle), tends to maintain the spherical shape of the particles. Deformation of particles results in elastic properties of the dispersed system. Graebing et al. [23] introduced viscoelasticity to describe the viscoelastic behavior of the particles and the medium over a wide frequency range. Palierne proposed an emulsion model that took into account the particle size distribution and the interface properties and arrived at the following expression [6]:

$$H_i(\omega) = \frac{\left( 4 \left( \frac{\alpha}{R_v} \right) (2G_m^*(\omega) + 5G_i^*(\omega)) + (G_i^*(\omega) - G_m^*(\omega)) (16G_m^*(\omega) + 19G_i^*(\omega)) \right)}{\left( 40 \left( \frac{\alpha}{R_v} \right) (G_m^*(\omega) + G_i^*(\omega)) + (2G_i^*(\omega) + 3G_m^*(\omega)) (16G_m^*(\omega) + 19G_i^*(\omega)) \right)}$$

$$G_b^*(\omega) = G_m^*(\omega) \frac{1 + 3 \int_0^\infty \frac{E(\omega, R)}{D(\omega, R)} \nu(R) dR}{1 - 2 \int_0^\infty \frac{E(\omega, R)}{D(\omega, R)} \nu(R) dR} \quad (3)$$

where

$$\begin{aligned} E(\omega, R) = & [G_i^*(\omega) - G_m^*(\omega)] [19G_i^*(\omega) + 16G_m^*(\omega)] \\ & + \frac{4\alpha}{R} [5G_i^*(\omega) + 2G_m^*(\omega)] \\ & + \frac{\beta_1^*(\omega)}{R} [23G_i^*(\omega) - 16G_m^*(\omega)] \\ & + \frac{2\beta_2^*(\omega)}{R} [13G_i^*(\omega) + 8G_m^*(\omega)] + \frac{24\beta_1^*(\omega)\alpha}{R^2} \\ & + 16\beta_2^*(\omega) \frac{\alpha + \beta_1^*(\omega)}{R^2} \end{aligned}$$

$$\begin{aligned} D(\omega, R) = & [2G_i^*(\omega) + 3G_m^*(\omega)] [19G_i^*(\omega) + 16G_m^*(\omega)] \\ & + \frac{40\alpha}{R} [G_i^*(\omega) + G_m^*(\omega)] \\ & + \frac{2\beta_1^*(\omega)}{R} [23G_i^*(\omega) + 32G_m^*(\omega)] \\ & + \frac{4\beta_2^*(\omega)}{R} [13G_i^*(\omega) + 12G_m^*(\omega)] + \frac{48\beta_1^*(\omega)\alpha}{R^2} \\ & + 32\beta_2^*(\omega) \frac{\alpha + \beta_1^*(\omega)}{R^2} \end{aligned}$$

$G_b^*(\omega)$  complex modulus of polymer blend;

$G_i^*(\omega)$  complex modulus of dispersed phase;

$G_m^*(\omega)$  complex modulus of matrix;

$\beta_1^*(\omega)$  surface dilatation modulus;

$\beta_2^*(\omega)$  surface shear modulus;

$R$  dispersed particle radius;

$\nu(R)$  distribution function of dispersed particle radius;

$\alpha$  interfacial tension;

$\omega$  angular frequency.

In the linear viscoelastic zone, the deformation of the dispersed particles is small. Thus, it is reasonable to assume that  $\beta_1^*(\omega) = \beta_2^*(\omega) = 0$ . As a result, if the particle size distribution of the dispersed phase is narrow enough ( $R_v/R_n \leq 2$ ), then Eq. (3) can be reduced to

$$G_b^*(\omega) = G_m^*(\omega) \frac{1 + 3 \sum_i \phi_i H_i(\omega)}{1 - 2 \sum_i \phi_i H_i(\omega)} \quad (4)$$

where

$R_v (R_v = \sum n_i R_i^4 / \sum n_i R_i^3)$ : volume average particle radius;

$R_n (R_n = \sum n_i R_i / \sum n_i)$ : number average radius.

Palierne emulsion model has been widely used to quantitatively describe the linear viscoelastic properties of polymer blends and to derive the interfacial tension from them [23,41,42]. However, it has to be modified when it comes to complex morphologies, such as emulsion-in-emulsion (EE) morphology in PS/PMMA blends [22]. The situation could be even more complicated with compatibilized polymer blends for which even experimental results themselves have been subject of controversy in the literature [34,36,43–46]. For example, unlike Riemann et al. [28,34] and Jacobs et al. [36], Velankar et al. [46] did not observe the expected slow interfacial relaxation process in the PDMS/PIB blends they investigated. Reasons for those discrepancies could be of different types. In most blends, the material responses did not cover the form relaxation region or the form relaxation processes were too slow to be within the experimental

frequency or time range [43,45]. In other cases [47,48], like the ‘salami type’ morphology that is formed in high impact polystyrene, particles were not uniform enough in size or their morphologies were too complex. Addition of block copolymers could also lead to complex morphologies [44,49]. There are also situations where the concentrations of the dispersed particles were too high to quantitatively apply the models [43,45] ( $> \sim 30$  vol%).

In a previous work [7], based on Palierne emulsion model, the experimentally measured data of the complex modulus of PP/PP-g-MAH/PA6 ternary blends were used to determine the interfacial tension between the PP/PP-g-MAH and the PA6. The EE morphology in the blends was taken into account. The value of the interfacial tension obtained was in good agreement with that reported in the literature [49,50] (the difference was less than 5%). However, to fit the model to the experimental data, the volume fraction of the dispersed phase had to be artificially increased with decreasing angular frequency, which did not have any physical foundations. Thus, the predictability of Palierne emulsion model was not really proven. In this work, the applicability of that model was further investigated by studying the terminal behavior (terminal relaxation time) of the polymer blends only in order to alleviate the above-mentioned problems. In that way, since emulsion-in-emulsion structures were much larger in size than particles of the dispersed phase, their terminal relaxation time was significantly beyond the time scale of our experiments.

## 2. Experiments

### 2.1. Materials

A polyamide 6 (PA6) was supplied by Heilongjiang Nylon Plastic Factory, China. Its relative viscosity was 2.5 (1 g/100 ml formic acid solution at 30 °C). An isotactic polypropylene (PP) was supplied by Beijing Yanshan Petrochemical Co. Ltd, China. A polypropylene grafted with maleic anhydride (PP-g-MAH) was supplied by Elf Atochem now Arkema, France. The MAH content was 1.03 wt% with respect to the PP. Table 1 shows other characteristics of those polymers.

### 2.2. Preparation of PP/PA6 and PP/PP-g-MAH/PA6 blends

Blends were prepared by using an internal mixer of type Brabender Plasticord PLE 330. Before blending, the PP, PP-g-MAH and PA6 were dried in a vacuum oven at 85 °C for 24 h. The mixing temperature was set at 230 °C. The

rotating speed of the rotors was 50 rpm. The mixing time was 7 min. In those blends, the PA6 was always the dispersed phase and the PP or PP+PP-g-MAH mixture was always the matrix.

### 2.3. Rheological measurement

Oscillatory rheological characterization of the blends was carried out at 230 °C on a Physica MCR-300 rheometer with a 25 mm parallel plate arrangement. Disks of 1 mm thick were prepared by compression-molding pellets in a hot press under 5 tons and at 230 °C. The pellets were pre-dried at 80 °C in a vacuum oven for 12 h. The rheometer oven was purged with dry nitrogen during measurement to avoid degradation. A frequency range of 0.01–100 rad/s and a strain of 5% were applied during the measurement. A strain sweep was carried out to determine the strain limit for the linear viscoelastic response range. The relaxation spectra were calculated by using a non-linear regression regularization method (NLREG) developed by Honerkamp and Weese [13]. The latter was available in the software package of Physica MCR-300 rheometer. Creep tests were also performed to evaluate the zero shear viscosity of each of the components of the blends [25,27] at 230 °C. The zero shear viscosity of the PA6, PP and PP-g-MAH at 230 °C were 1250, 1300 and 50 Pa s, respectively.

### 2.4. Morphology analysis

The morphologies of the PP/PA6 uncompatibilized blends were observed with a Jeol JXA-840 scanning electron microscope (SEM). In order to have a better contrast, samples were fractured in liquid nitrogen, etched by formic acid to remove the PA6 particles. They were then coated with 50/50 Au/Pt to avoid charging. Those of the PP/PP-g-MAH/PA6 compatibilized blends were characterized by using the SEM and a JEOL-2010 transmission electron microscope (TEM), respectively. The TEM elastic bright-field images were taken. The accelerating voltage was 200 keV. Ultrathin films of about 60 nm in thickness were obtained from quenched discs using a Leica Ultracut-E microtome with a diamond knife. They were treated with RuO<sub>4</sub> vapor in order to improve the contrast [51,52]. Since, the staining rate of the PP phase was slower than that of the PA6, the PA6 domains appeared darker than the PP. The radius of the particles was determined from several representative photographs.

Table 1  
Characteristics of the PA6, PP and PP-g-MAH

Polymer	$\bar{M}_n$ (kg/mol)	$\bar{M}_w$ (kg/mol)	$d$ (25 °C) (g/cm <sup>3</sup> )	MFR 230 °C (g/10 min)	Zero shear viscosity at 230 °C (Pa s)	Relaxation time <sup>a</sup> at 230 °C (s)
PA6	24.0	–	1.14	–	1250	0.03
PP	65.0	259.0	0.902	7.9	1300	0.35
PP-g-MAH	59.0	320.0	0.902	100	50	0.25

<sup>a</sup> Obtained from the main peak value in the relaxation time spectra of the polymers.

Table 2  
Average particle radii and particle polydispersities of the PP/PP-g-MAH/PA6 compatibilized blends

PP/PP-g-MAH/PA6	$\phi_{PA6}^a$ (%)	$R_v$ ( $\mu\text{m}$ )	$R_n$ ( $\mu\text{m}$ )	$R_v/R_n$
90/0/10	8.1	3.5	2.2	1.6
70/0/30	25.4	17.7	7.5	2.4
45/45/10	8.1	0.11	0.08	1.3
35/35/30	25.4	0.2	0.1	2.0
80/10/10	8.1	0.13	0.11	1.3
60/10/30	25.4	0.3	0.2	1.5

<sup>a</sup> The volume fractions of the PA6 in the blends were calculated based on the following specific masses:  $\rho_{PP}=0.902 \text{ g/cm}^3$ ,  $\rho_{PA6}=1.14 \text{ g/cm}^3$ .

### 3. Results and discussion

#### 3.1. Theoretical background

Before we begin to present the experimental results, it would be useful to outline the theoretical bases we used in this work. Using the continuous representation of the Maxwell model, the relaxation spectrum  $H(\lambda)$  is related to  $G'$  and  $G''$  through the Fredholm integral equation of the first kind [21]:

$$t_1 = \frac{R_v \eta_m}{4\alpha} \frac{(19K + 16)(2K + 3 - 2\phi_i(K - 1))}{10(K + 1) + \frac{\beta_{20}}{\alpha}(13K + 12) - \phi_i[2(5K + 2) + \frac{\beta_{20}}{\alpha}(13K + 8)]}$$

$$t_2 = \frac{R_v \eta_m}{4\beta_{20}} \frac{10(K + 1) + (\beta_{20}/\alpha)(13K + 12) - \phi_i[2(5K + 2) + (\beta_{20}/\alpha)(13K + 8)]}{1 - \phi_i}$$

$$G'(\omega) = \int_{-\infty}^{+\infty} \frac{\omega^2 \lambda^2}{1 + \omega^2 \lambda^2} H(\lambda) d(\ln \lambda) \quad (5)$$

$$G''(\omega) = \int_{-\infty}^{+\infty} \frac{\omega \lambda}{1 + \omega^2 \lambda^2} H(\lambda) d(\ln \lambda) \quad (6)$$

where  $\lambda$  is the relaxation time.

After an oscillation test, a relaxation time spectrum can be calculated from the storage modulus data of the blends using the NLREG method [13]. The peak values of the relaxation time spectrum are called experimental relaxation times of a blend. On the other hand, the form relaxation time of the dispersed phase can be predicted by Palierne emulsion model [6]. If the variations of the interface area and interface relaxation are ignored and both the dispersed and continuous phases are assumed to be Newtonian fluids, which are valid when the angular frequency is very low, the form relaxation time can be calculated from Eq. (7):

$$\tau_1 = \frac{R_v \eta_m}{4\alpha} \frac{(19K + 16)(2K + 3 - 2\phi_i(K - 1))}{10(K + 1) - 2\phi_i(5K + 2)} \quad (7)$$

If the interface relaxation is taken into account,  $\beta_2^*$  in Eq. (3) is no longer zero but  $\beta_2^* = \beta_{20}$ . The form relaxation time can then be calculated by Eq. (8) [28]:

$$\tau_\beta = \frac{t_2}{2} \left[ 1 + \left( 1 - 4 \frac{t_1}{t_2} \right)^{1/2} \right] \quad (8)$$

with:

For  $\beta_{20} \rightarrow 0$ , i.e. for uncompatibilized blends, Eq. (8) is reduced to Eq. (7). The relaxation times calculated by Eqs. (7) and (8) are called theoretical terminal relaxation times. In this work, the latter were compared with experimental ones. Differences between them were analyzed in detail.

#### 3.2. Morphology

Rheological and other physical properties of polymer blends are closely related to the dispersion and distribution of the

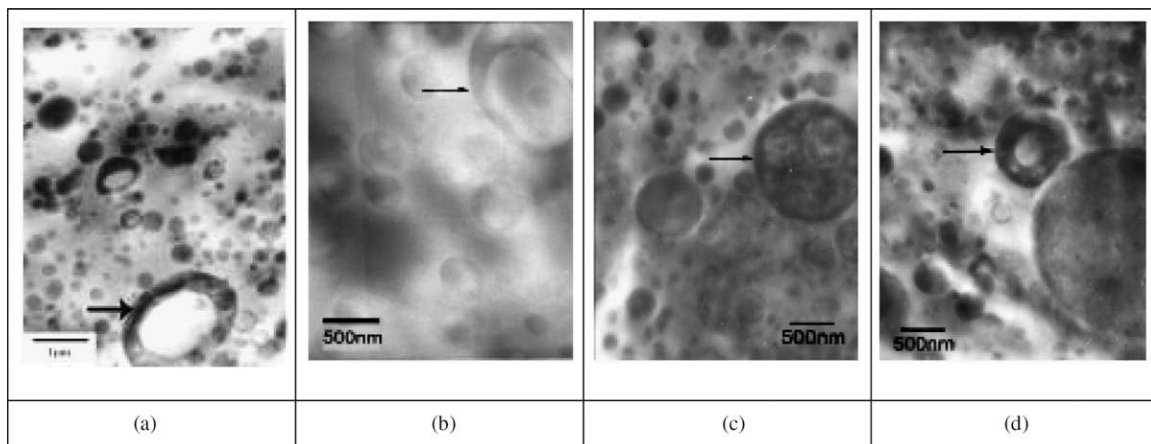


Fig. 1. Emulsion-in-emulsion structures in compatibilized PP/PP-g-MAH/PA6 blends: (a) 80/10/10; (b) 45/45/10; (c) 35/35/30; (d) 60/10/30.

particles of the dispersed phase in the matrix. Therefore, it is essential to determine the sizes of the particles and their distribution in the blends in order to interpret rheological data and assess rheological models. Table 2 lists the number average radius  $R_n$  and volume average radius  $R_v$ , of the particles of various blends studied in this work. The compatibilized blends showed EE structures, as indicated by arrows in Fig. 1. Those structures were excluded from the calculation of  $R_v$  and  $R_n$ . This is because as already mentioned above, we studied the terminal behavior (terminal relaxation time) of the polymer blends only and the terminal relaxation times of the EE structures were beyond the experimental time scale.

The radii of the PA6 domains were of the order of 10  $\mu\text{m}$  for the uncompatibilized blends [7] and were in the submicrometer range for the compatibilized ones. The particle size distributions of the uncompatibilized blends were broader than those of the compatibilized ones.

Consider now how the EE structures were formed in the PP/PP-g-MAH/PA6 compatibilized blends. The PP and PP-g-MAH used in this work were supposed to be miscible under the

processing conditions (Appendix A). Thus, a PP/PP-g-MAH/PA6 blend could initially be considered as a two-phase system: PP/PP-g-MAH matrix and the PA6 dispersed phase. Under mixing, PP-g-PA6 graft copolymers were formed at the interfaces between the PP-g-MAH and the PA6. For mechanical and/or thermodynamic reasons, they could be pulled out from the interfaces where they were generated [53] and then formed micelles in the PA6 particles [54] and/or the

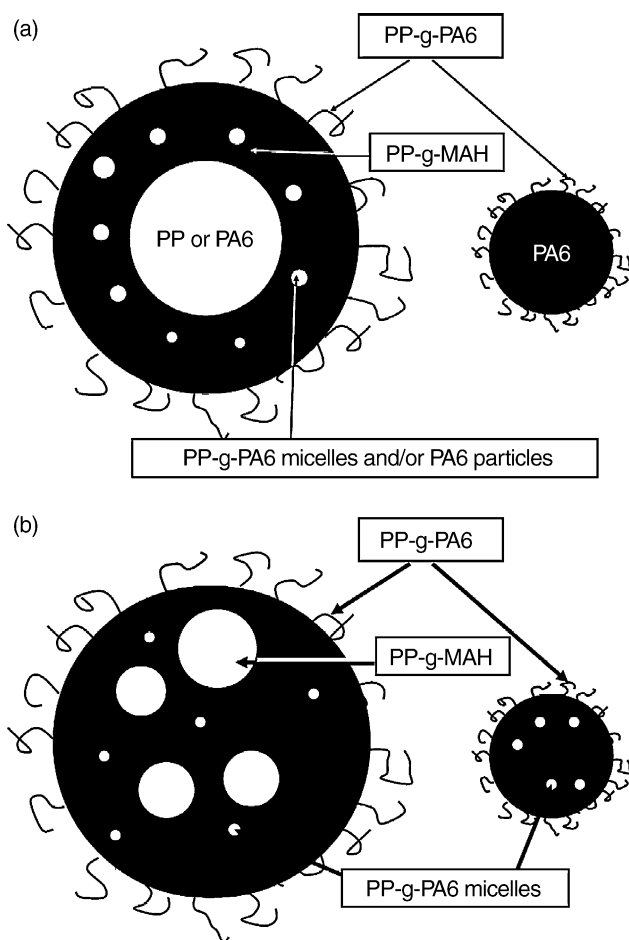


Fig. 2. Schematics of emulsion-in-emulsion structures in PP/PP-g-MAH/PA6 compatibilized blends. (a) PP or PA6 particles were encapsulated by PP-g-MAH. This type of structure is likely possible when the PP-g-MAH or PA6 content is relatively high or both of them are low; (b) PP-g-MAH droplets encapsulated by large PA6 particles. This type of structure may likely exist when both the PP-g-MAH and PA6 contents are relatively high.

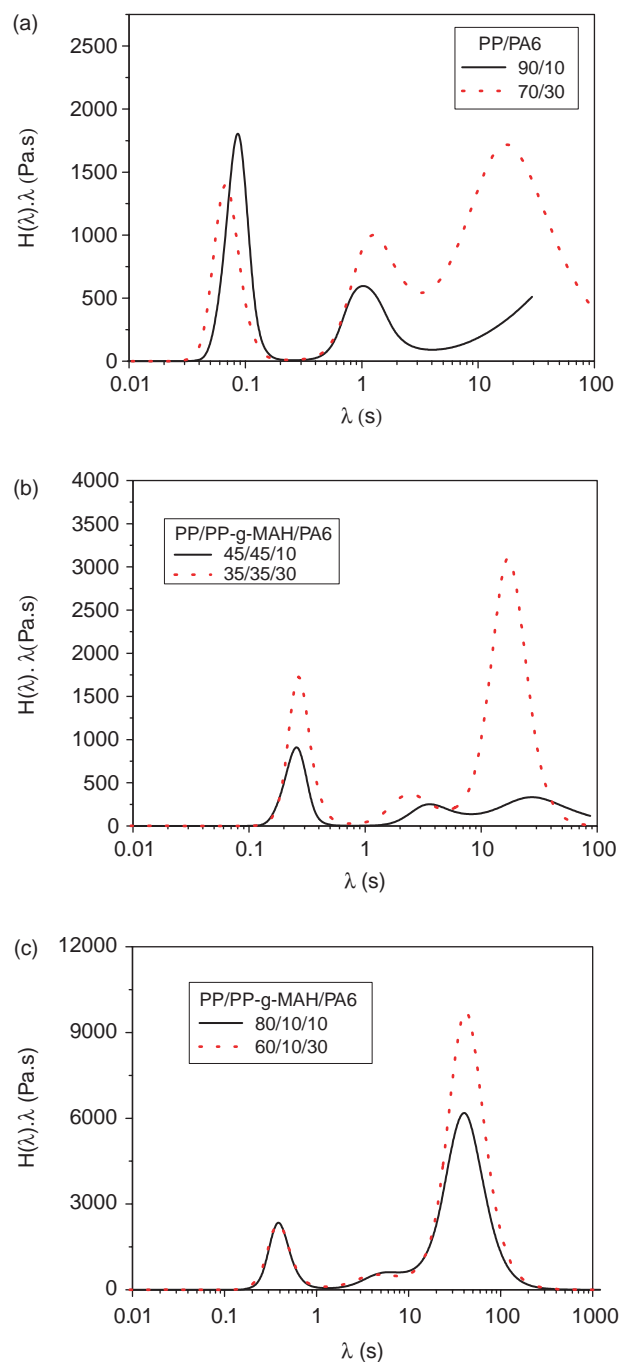


Fig. 3. Relaxation time spectra of PP/PA6 uncompatibilized blends and PP/PP-g-MAH/PA6 compatibilized blends of varying PA6 contents at 230 °C. (a) PP/PA6 uncompatibilized blends; (b) PP/PP-g-MAH/PA6 compatibilized blends with higher PP-g-MAH contents; (c) PP/PP-g-MAH/PA6 blends with lower PP-g-MAH contents.

PP/PP-*g*-MAH matrix [55,56]. The dissolution of the PP-*g*-PA6 micelles in the PP/PP-*g*-MAH matrix could increase the interaction parameter between the PP and PP-*g*-MAH and cause a phase separation between the PP and PP-*g*-MAH (Ref. [7] for supporting information). Since, PP-*g*-MAH had a much lower viscosity than the PP and PA6, it tended to encapsulate the PP or PA6 particles when EE structures were formed (Fig. 1(a), (b) and (d)). However, when the amounts of the PP-*g*-MAH and PA6 were relatively large, the excess of the PP-*g*-MAH could be located inside the PA6 particles forming another type of EE structures [22] (Fig. 1(c)).

Fig. 2 shows in a schematic manner that two types of EE structures can be formed in the PP/PP-*g*-MAH/PA6 compatibilized blends. In addition to neat PA6 particles, there are also EE structures in the PP/PP-*g*-MAH matrix. Both the neat PA6 particles and the EE structures are surrounded by the PP-*g*-PA6 graft copolymers. The latter could also be located in these two types of particles in the form of micelles.

### 3.3. Rheology

Fig. 3 shows the relaxation time spectra of various PP/PA6 uncompatibilized blends and PP/PP-*g*-MAH/PA6 compatibilized blends calculated directly from the storage modulus data obtained by the oscillation tests. The two peaks at shorter times resulted from the matrix relaxation. The third peak at the longest time corresponded to the form relaxation time. However, no form relaxation time peak was observed for the PP/PA6 (90/10) uncompatibilized blend, likely because the form relaxation process of the dispersed phase merged with that of the matrix [26,32]. Table 3 gathers both the experimental and theoretical terminal relaxation times of all the blends. The value of the interfacial tension used for the theoretical predictions was 9.2 and 2.0 mN/m for the uncompatibilized and compatibilized blends, respectively. The value of  $\beta_{20}$  used to calculate  $\tau_\beta$  of the compatibilized blends was 0.02 mN/m. All those values were taken from Ref. [7].

For the PP/PA6 uncompatibilized blends, both the theoretical and experimental relaxation times matched well when the PA6 content was low, 10 wt%. However, when the latter was increased to 30 wt%, they differed greatly. At that high PA6

Table 3  
Relaxation times of the PP/PA6 uncompatibilized blends and PP/PP-*g*-MAH/PA6 compatibilized blends

PP/PP- <i>g</i> -MAH/PA6 by mass	$\tau$ (s) (Experimental)	$\tau$ (s) (Theoretical)	
		$\tau_1$ (Eq. (7))	$\tau_\beta$ (Eq. (8)) <sup>a</sup>
90/0/10	1.1	1.1 <sup>b</sup>	–
70/0/30	17.3	5.9 <sup>b</sup>	–
45/45/10	26.0	0.1 <sup>c</sup>	21.1
35/35/30	17.0	0.1 <sup>c</sup>	36.5
80/10/10	40.0	0.2 <sup>c</sup>	37.1
60/10/30	42.0	0.5 <sup>c</sup>	84.1

<sup>a</sup>  $\alpha = 2$  mN/m;  $\beta_{20} = 0.02$  mN/m.

<sup>b</sup>  $\alpha = 9.2$  mN/m.

<sup>c</sup>  $\alpha = 2$  mN/m.

content, PA6 particles were no more isolated but more or less interconnected [35]. As such, the Palierne model did not apply [26]. As for the PP/PP-*g*-MAH/PA6 compatibilized blends, the differences between the theoretical and experimental relaxation times were always large, irrespective of the PA6 content or the interfacial properties that were used for the calculations.

According to the morphologies of the PP/PP-*g*-MAH/PA6 compatibilized blends in Fig. 1, when the PA6 content was low (10 wt%), the existence of EE structures was responsible for the failure of the Palierne model. When it was high (30 wt%), overlap of the particles of the dispersed phase further contributed to its failure. In what follows, we will only show that for the compatibilized blend with a low PA6 content (10 wt%), Palierne emulsion model can satisfactorily predict its relaxation time if the EE structures are taken into account in an appropriate manner.

The size of the EE structures was much larger than that of the neat PA6 particles. Therefore, their terminal relaxation time was expected to be so long that it became inaccessible by the oscillating frequencies used in this work. However, they could affect the relaxation time of the neat PA6 particles because their presence in the PP/PP-*g*-MAH was expected to increase the viscosity of the matrix and decrease the volume fraction of the neat PA6 particles. If Palierne emulsion model is used to predict the form relaxation times of the neat PA6 particles, the viscosity of the medium (PP/PP-*g*-MAH + EE structures) and the volume fraction of the neat PA6 particles will have to be calculated.

Thus, to calculate the viscosity of the matrix of the PP/PP-*g*-MAH/PA6 compatibilized blend containing 10 wt% PA6, the EE structures in the PP/PP-*g*-MAH matrix should be taken into consideration. Based on the structures in Fig. 2(a) and assuming the matrix be a dilute emulsion system, Eq. (2) can be expressed as:

$$\eta_{0,m} = \eta_{0,PP/PP-g-MAH} \left[ 1 + \phi_1 \frac{5K_1 + 2}{2(K_1 + 1)} + \phi_1^2 \frac{(5K_1 + 2)^2}{10(K_1 + 1)^2} \right] \quad (9)$$

where  $\eta_{0,PP/PP-g-MAH}$  is the viscosity of the PP/PP-*g*-MAH mixture,  $\phi_1$  is the volume fraction of EE structures in the PP/PP-*g*-MAH medium and  $K_1 = \eta_{EE}/\eta_{0,PP/PP-g-MAH}$ .

Meanwhile, an EE structure itself could also be considered as a dilute emulsion system with PA6 particles dispersed in the PP-*g*-MAH. Thus, Eq. (2) was used to calculate its viscosity,  $\eta_{EE}$ :

$$\eta_{EE} = \eta_{0,PP-g-MAH} \left[ 1 + \phi_2 \frac{5K_2 + 2}{2(K_2 + 1)} + \phi_2^2 \frac{(5K_2 + 2)^2}{10(K_2 + 1)^2} \right] \quad (10)$$

where  $\eta_{0,PP-g-MAH}$  is the viscosity of the PP-*g*-MAH,  $\phi_2$  is the volume fraction of the PP or PA6 droplets in the EE structures. Since, the zero shear viscosities of the PA6 and PP were very close, the value of  $K_2$  was approximated as  $K_2 = \eta_{0,PA6}/\eta_{0,PP-g-MAH}$ . The effect of the PP-*g*-PA6 micelles on the shear viscosity was ignored.

According to Fig. 2(a),  $\phi_1$  in Eq. (9) and  $\phi_2$  in Eq. (10) can easily be expressed as follows:

$$\phi_1 = \frac{\varphi_{EE}}{\varphi_{EE} + \varphi_{PP}^{\text{residue}} + \varphi_{PP-g-MAH}^{\text{residue}}} \quad (11)$$

$$\phi_2 = \frac{\varphi_{PA}^d}{\varphi_{EE}} \quad (12)$$

where  $\varphi_{EE}$ ,  $\varphi_{PP}^{\text{residue}}$ ,  $\varphi_{PP-g-MAH}^{\text{residue}}$  and  $\varphi_{PA}^d$ ,  $\varphi_{PP-g-MAH}^{\text{residue}}$  are the volume fractions of the EE structures, the PP in the matrix, the PP-g-MAH in the matrix and the PA6 in the EE structures, respectively. The volume fractions of the neat PA6 droplets in the whole system ( $\phi_i$  in Eq. (8)), as well as  $\varphi_{PP}^{\text{residue}}$ ,  $\varphi_{PP-g-MAH}^{\text{residue}}$  and  $\varphi_{PP-g-MAH}^{\text{residue}}$  can then be expressed by:

$$\phi_i = \varphi_{PA}^0 - \phi_1 \phi_2 (1 - \phi_i) = \frac{\varphi_{PA}^0 - \phi_1 \phi_2}{1 - \phi_1 \phi_2} \quad (13)$$

$$\varphi_{PP-g-MAH}^{\text{residue}} = \varphi_{PP-g-MAH}^0 - (1 - \phi_i)[\phi_1 \times (1 - \phi_2)] \quad (14)$$

$$\varphi_{PP}^{\text{residue}} = \varphi_{PP}^0 - (1 - \phi_i)\phi_1 \phi_2 \quad (15)$$

where  $\varphi_{PP}^0$ ,  $\varphi_{PP-g-MAH}^0$  and  $\varphi_{PA}^0$  are the initial nominal volume fractions of the PP, PP-g-MAH and PA6 in the compatibilized blends, respectively. Eqs. (9)–(15) indicate that the matrix viscosity  $\eta_{0,m}$  is a function of  $\phi_1$  and  $\phi_2$ . However, the values of those two volume fractions were unknown and were not be able to quantify experimentally. In this work, their values were identified by searching for a set of values for  $\phi_1$ ,  $\phi_2$  and  $\eta_{0,m}$  that allowed the relative errors to be less than 1% between the calculated and experimental values in terms of the form relaxation times of the neat PA6 particles.

Table 4 lists the values of those three parameters that met the above criterion for the PP/PP-g-MAH/PA6 compatibilized blends with 10 wt% PA6 (45/45/10 and 80/10/10). The volume fractions of the neat PA6 particles in the blends were smaller than the initial PA6 contents. Moreover, it decreased with increasing initial PP-g-MAH content. Those results seem to be logical and could be understood as follows. During the reactive blending process, the reaction between the PP-g-MAH and PA6 led to the formation of the PP-g-PA6 graft copolymer. As a result, after blending the volume fractions of the neat PA6 in the polymer blends should be smaller than its initial nominal ones. Moreover, the higher the initial PP-g-MAH content in the blend, the more the PA6 was expected to react with the PP-g-MAH, the more the PA6 could be encapsulated by the EE structures and the less the volume fraction of the neat PA6 in

the blend should be. On the other hand, the viscosity of the matrix should increase with increasing volume fraction of the EE structures in the blend. Thus we could conclude that the methodology developed in this work could be used for applying the Palierne model to predict rheological properties of polymer blends with complex morphologies such as the PP/PP-g-MAH/PA6 compatibilized blends.

#### 4. Conclusion

In this work, the dynamic rheological behavior of polypropylene/polyamide6 (PP/PA6) uncompatibilized blends and those compatibilized with a maleic anhydride grafted PP (PP/PP-g-MAH/PA6) was studied. The terminal relaxation times of the blends predicted by Palierne emulsion model were compared with those obtained from experimental relaxation time spectra. The model succeeded well in describing PP/PA6 uncompatibilized blends with relatively low dispersed phase contents (10 wt%) and failed doing so for those of which the dispersed contents were high (30 wt%). It also failed for the compatibilized ones, irrespective of the dispersed phase content (10 or 30 wt%) and whether or not the interface relaxation was taken into consideration. In the case of the uncompatibilized blend with high dispersed-phase content, interconnections among inclusions of the dispersed phase were responsible for the failure of the Palierne model. As for the compatibilized blends, in addition to particle interconnections, the existence of emulsion-in-emulsion structures was another factor responsible for the failure of Palierne model. When the effects of the emulsion-in-emulsion structure on the viscosity of the continuous phase and the effective volume fraction of the dispersed phase were properly taken into account, the model worked well again. This indicates that Palierne emulsion model can be used to predict rheological properties of polymer blends with complex morphologies provided that the latter are properly described.

#### Acknowledgements

This work was supported by the National Science Foundation of China through a Major Program (50390090) and a General Program (50373011), the Wuhan Youth Scheme of Science and Technology (20025001012), the Research Grants Council of the Hong Kong Special Administrative Region, China (Project No. CityU 1202/02E) and the Fédération de Recherche Jacques Villermaux (CNRS FR 2863) (Project: Rheology and Interface in dispersed media).

#### Appendix A

In our previous work [7], we showed that the PP and PP-g-MAH used in our work was miscible at 230 °C by calculating the interaction parameter between them. Here, we present the other evidence. Table A1 lists the zero shear viscosities of the PA6, PP, PP-g-MAH and mixtures of the PP and PP-g-MAH. We can find that the experimental data agrees well with the

Table 4

Identified values of  $\phi_1$ ,  $\phi_2$ ,  $\varphi_{PA}^{\text{neat}}$  and  $\eta_m$  that allowed the relative errors between the experimental relaxation times and those predicted by the Palierne model to be less than 1%

PP/PP-g-MAH/PA6	$\phi_1$	$\phi_2$	$\varphi_{PA}^{\text{neat}}$	$\eta_{0,m}$ (Pa s)	$\eta_m^a$ (Pa s)
45/45/10	0.31	0.13	0.05	604	255
80/10/10	0.05	0.3	0.07	1052	905

<sup>a</sup> Matrix viscosity before modification.

Table A1  
Zero shear viscosities of blend components

Polymer material	$\eta_0$ at 230 °C (Pa s)	$\eta_0^a$ (Pa s)
PA6	1250	
PP	3000	
PP-g-MAH	301	
PP/PP-g-MAH (50/50)	950	950
PP/PP-g-MAH (80/10)	2300	2324
PP/PP-g-MAH (70/10)	2260	2251
PP/PP-g-MAH (60/10)	2180	2160

$\eta_0^a$  Calculated by the Irving additive equation [57] ( $\log \eta = \sum_i \phi_i \log \eta_i$ ) for miscible polymer blends.

Irving equation. These results indicate that PP/PP-g-MAH pairs employed in our work are miscible at 230 °C.

## References

- [1] Paul DR, Newman S. Polymer blends, vols. 1 and 2. Academic Press: New York; 1976.
- [2] Utracki LA, Weiss RA. Multiphase polymers: blends and ionomers. Washington DC: ACS; 1989.
- [3] Utracki LA, editor. Two-phase polymer systems. Macrochem: Hanser Verlag; 1991.
- [4] Sanchez IC, Fitzpatrick LE, editors. Physics of polymer surfaces and interfaces. Boston: Butterworth-Heinemann; 1992.
- [5] Wu S. Polymer interfaces and adhesion. New York and Basel: Marcel Dekker Inc.; 1982.
- [6] Paliere JP. Rheol. Acta 1990;29:204–14.
- [7] Shi D, Yang JH, Ke Z, Gao Y, Wu J, Yin JH. Macromolecules 2002;35:8005.
- [8] Baumgaertel M, Winter HH. Rheol Acta 1989;28:511.
- [9] Baumgaertel M, Winter HH. J Non-Newtonian Fluid Mech 1992;44:15.
- [10] Honerkamp J, Weese J. Macromolecules 1989;22:4372.
- [11] Elster C, Honerkamp J. Macromolecules 1991;24:310.
- [12] Honerkamp J, Weese J, Elster C. Rheol Acta 1991;30:161.
- [13] Honerkamp J, Weese J. Rheol Acta 1993;32:65.
- [14] Lee CY-C, Wiff DR, Rodgers VGJ. Macromol Sci-Phys 1981;B19(2):211.
- [15] Mead DW. J Rheol 1994;38:1769.
- [16] Ramkumar DHS, Caruther JM, Mavridis H, Shroff RJ. Appl Polym Sci 1997;64:2177.
- [17] Emri L, Tschoegl NW. Rheol Acta 1993;32:311.
- [18] Emri L, Tschoegl NW. Rheol Acta 1994;33:60.
- [19] Brabec CJ, Schausberger A. Rheol Acta 1995;34:397.
- [20] Brabec CJ, Rögl H, Schausberger A. Rheol Acta 1997;36:667.
- [21] Ferry JD. Viscoelastic properties of Polymers. New York: John Wiley & Sons Inc.; 1980.
- [22] Fahrlander M, Friedrich C. Rheol Acta 1999;38:206–13.
- [23] Graebing D, Muller R, Paliere JP. Macromolecules 1993;26:320–9.
- [24] Peón J, Vega JF, Del Amo B, Martínez-Salazar J. Polymer 2003;44:2911–8.
- [25] Kraft M, Meissner J, Kaschta J. Macromolecules 1999;32:751–7.
- [26] Souza AMC, Demarquette NR. Polymer 2002;43:1313–21.
- [27] Macaúbas PHP, Demarquette NR. Polymer 2001;42:2543–54.
- [28] Riemann RE, Cantow HJ, Friedrich C. Macromolecules 1997;30:5476–84.
- [29] Matsumoto T, Hori N, Takahashi M. Langmuir 1996;12:5563–9.
- [30] Doi M, Ohta T. J Chem Phys 1991;95(2):1242–8.
- [31] Van Hemelrijck E, Van Puyvelde P, Velankar S, Macosko CW, Moldenaers P. J Rheol 2004;48:143–58.
- [32] Lacroix C, Aressy M, Carreau PJ. Rheol Acta 1997;36:416–28.
- [33] Sung YT, Han MS, Hyun JC, Kim WN, Lee HS. Polymer 2003;44:1681–7.
- [34] Riemann RE, Cantow HJ, Friedrich C. Polym Bull 1996;36:637–43.
- [35] Hu GH, Li H, Feng LF. AIChE J 2002;48:2620–8.
- [36] Jacobs U, Fahrlander M, Winterhalter J, Friedrich C. J Rheol 1999;43:1495–509.
- [37] Taylor GI. Proc R Soc London 1932;A1(32):41.
- [38] Oldroyd JG. Proc R Soc London, Ser A 1953;218:122.
- [39] Schowalter WR, Chaffey CE, Brenner H. J Colloid Interface Sci 1967;26:152.
- [40] Scholz P, Froelich D, Muller R. J Rheol 1989;33:481.
- [41] Friedrich Chr, Gleinser W, Korat E, Maier D, Weese J. J Rheol 1995;39:1411.
- [42] Lacroix C, Bousmina M, Carreau PJ, Favis BD, Michel A. Polymer 1996;37:2939.
- [43] Germain Y, Ernst B, Genelot O, Dhamani L. J Rheol 1994;38:681.
- [44] Riemann R-E, Braun H, Weese J, Schneider HA. New Polym Mater 1994;4:131.
- [45] Kim HC, Nam KH, Jo WH. Polymer 1993;34:4043.
- [46] Velankar S, Van Puyvelde P, Mewis J, Moldenaers P. J Rheol 2001;45:1007–19.
- [47] Gleinser W, Braun H, Friedrich Chr, Cantow H-J. Polymer 1994;35:128.
- [48] Brahimi B, Ait-Kadi A, Aji A, Jerome R, Fayt R. J Rheol 1991;35:1069.
- [49] Haaga S, Friedrich Chr. Polym Networks Blends 1994;4:61.
- [50] Asthana H, Jayaraman K. Macromolecules 1999;32:3412–9.
- [51] Trent JS, Scheinbeim JI, Couchman PR. Macromolecules 1983;16:589.
- [52] Montezinos D, Wells BG, Burns JL. J Polym Sci, Polym Chem Ed 1985;23:421.
- [53] Pan LH, Chiba T, Inoue T. Polymer 2001;42:8825–31.
- [54] Charoensirisomboon P, Chiba T, Inoue T, Weber M. Polymer 2000;41:5977–84.
- [55] Jeon HK, Kim JK. Macromolecules 1998;31:9273–80.
- [56] Oyama HT, Inoue T. Macromolecules 2001;34:3331–8.
- [57] Irving JB. Viscosity of binary liquid mixture: a survey of mixture equation. Report No. 630. East Kilbridge, Glasgow, UK: National Engineering Laboratory; 1977.